journal

J. Am. Ceram. Soc., 81 [10] 2677–86 (1998)

Morphology of Silicon Nitride Grown from a Liquid Phase

Ling-Ling Wang and Tseng-Ying Tien*

Department of Materials Science and Engineering, University of Michigan, Ann Arbor, Michigan 48109–2136

I-Wei Chen*,†

Department of Materials Science and Engineering, University of Pennsylvania, Philadelphia, Pennsylvania 19104–6272

To explain the recent experimental observation of liquid-grown silicon nitride (Si_3N_4) crystals with a concave depression in the center of the (0001) end face, we propose a new growth mechanism and develop an analytical solution for the steady state. The model allows for atoms that diffuse via the liquid to the side surface but demands that the majority of these atoms be transported to the end caps to feed axial growth. The analysis shows that, for a large radius crystal, the redistribution of atoms by surface diffusion on the end caps requires a long relaxation time; hence, a nonequilibrium shape results. For an isolated Si_3N_4 crystal growing in a liquid environment, the shape of the end cap is largely determined by the ratio of the supersaturation to the equilibrium surface potential, which is inversely proportional to the crystal radius. A large shape distortion is predicted to occur during the growth stage for large-radius crystals and during the coarsening stage for a population of crystals with a large size distribution. This mechanism ceases to operate when the liquid flux to the side surface is blocked, as in silicon nitride ceramics, but is otherwise insensitive to factors such as radial growth kinetics and liquid diffusivity.

I. Introduction

ANISOTROPIC grain growth is an important feature that makes silicon nitride (Si_3N_4) a tough ceramic.[1–3] Si_3N_4 is sintered using additives that form a liquid.[4–12] Usually, β-Si_3N_4 grains grown from the liquid are faceted hexagonal cylinders, aligned in the (0001) directions with prismatic ($1\bar{1}00$) side faces.[13–16] The ends of the cylinder have a rounded shape.[13–16] Transmission electron microscopy (TEM) examinations of these surfaces further suggest an atomically flat interface on the side, with occasional ledges and an atomically rough interface at the ends.[17,18] Because atomically rough interfaces are expected to have little difficulty in accepting and accommodating new atoms (compared to atomically flat interfaces), the anisotropic growth of Si_3N_4 has been attributed to different growth kinetics on (0001) and ($1\bar{1}00$) surfaces.[18–20] The attention of researchers in the last decade has been focused on whether it is the diffusion in the liquid or the attachment on the interface that is the rate-controlling step in the growth kinetics.[19–24]

A recent model experiment on β-Si_3N_4 crystals grown from a liquid with alumina (Al_2O_3), yttria (Y_2O_3), and magnesia (MgO) additives revealed a very different picture.[25] As shown in Fig. 1, the shape of the end cap of the hexagonal β-Si_3N_4 grains can be convex or concave, depending on the width of the cross section. These crystals are well separated in the liquid, which contains only a small (15 vol%) fraction of solid, so that the interference of the diffusion field between the crystals is not a serious concern. The above-mentioned observation suggests a new transport mechanism that has been previously overlooked; namely, the atoms are first collected on the side surface and then transported through the edge of the end cap to the end surface. This mechanism can be inferred by comparing the curvature, hence the chemical potential, of the surface at different points on the end cap. Referring to Fig. 1, we see that the edge of the cap has a convex curvature and a positive chemical potential, whereas the center of the cap has a concave curvature and a negative chemical potential. Thus, a radially inward atomic flux must flow from the edge to the center. A continuity of fluxes, in turn, implies material transport from the side surfaces to the edge.

The two growth modes of the end face—(i) liquid diffusion from the surroundings and (ii) surface diffusion from the edge—are additive to each other. For a shape such as that in Fig. 1, with the chemical potential at the center much lower than that at the edge, the liquid-diffusion mode will have a tendency to smooth out the curvature difference and restore a spherical cap shape as it grows. On the other hand, if the source of atoms is primarily from the edge, then the curvature difference must continue, to sustain the driving force for surface diffusion. Indeed, the larger the flux of matter from the edge, the larger the curvature difference. The observation that such shapes do exist suggests that the surface mode is the dominant form of atomic transport. It then follows that the shape evolution in the same liquid is dependent on the width of the cylindrical crystal, because surface curvature generated by surface diffusion is known to be strongly size dependent, as observed in such phenomena as grain-boundary grooving,[26] Rayleigh instability,[27–30] and creep cavitation.[31–34]

To better understand the morphology of Si_3N_4 and to guide future experiments, we have undertaken a theoretical analysis of the kinetics of axial growth in a liquid environment. For simplicity, we will assume that the cylindrical crystal has a circular cross section and solve the steady-state problems first. It will be shown that these simplified solutions provide an adequate description of the experimentally observed shape evolution. Although the radial growth is initially ignored in the analysis, its incorporation will be considered in the Discussion section. The effect of a higher volume fraction of solid that forces the impingement of grain will also be discussed, to bring the present analysis into contact with the observed growth kinetics in silicon nitride ceramics.

D. R. Clarke—contributing editor

Manuscript No. 190841. Received July 16, 1997; approved January 14, 1998.

Supported by the U.S. Department of Energy, under Contract No. DE-AC05-84 OR22464, and by the Air Force Office of Scientific Research, under Grant No. AFOSR-G-F49620-98-1-0126.

Presented at the 99th Annual Meeting of the American Ceramic Society, May 4–7, 1997, Cincinnati, OH (Paper No. B-031-97).

*Member, American Ceramic Society.

†Author to whom correspondence should be addressed.

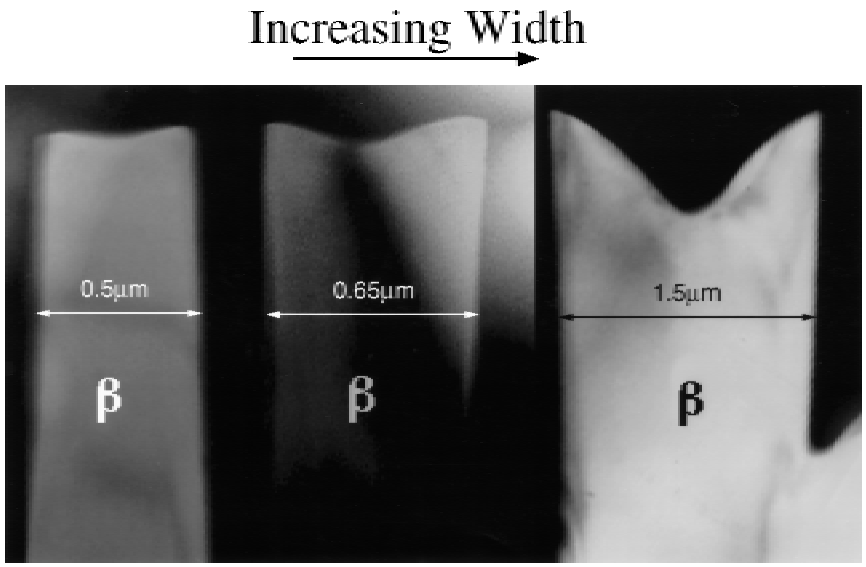

Fig. 1. Si_3N_4 crystals grown from a melt containing Si_3N_4, Al_2O_3, Y_2O_3, and MgO at 1600°C for 2 h in 10 atm of nitrogen gas; the solid fraction of Si_3N_4 is 15 vol%, to minimize crystal impingement.

II. Shape of End Caps

(1) Equilibrium Shape

We first solve the equilibrium shape of a cylindrical rod with two spherical caps at the ends, assuming knowledge of the surface energies. The chemical potential of a surface atom is given by

$$\mu = -\gamma\Omega(\kappa_1 + \kappa_2) \tag{1}$$

where κ_1 and κ_2 are principal curvatures (negative for a convex body) of the surface and γ is the surface energy.[31] We assume the side of the cylindrical rod is straight, with a radius a, and the surface energy is independent of orientation, given by $\gamma_\perp$. Then, the chemical potential of a surface atom on the side is

$$\mu_\perp = \frac{\gamma_\perp\Omega}{a} \tag{2}$$

We also assume that the spherical cap has a radius b and the surface energy is isotropic, given by $\gamma_\parallel$. Then, the chemical potential of a surface atom at the end is

$$\mu_\parallel = \frac{2\gamma_\parallel\Omega}{b} \tag{3}$$

At equilibrium, these two chemical potentials are the same and equal to the equilibrium surface chemical potential $\mu°$. Thus,

$$\frac{a}{b} = \frac{\gamma_\perp}{2\gamma_\parallel} \tag{4}$$

Referring to Fig. 2, it is also clear that

$$\sin\chi = \frac{a}{b} \tag{5}$$

where χ is the angle made between the spherical cap and a flat end. Thus,

$$\chi = \sin^{-1}\left(\frac{a}{b}\right) = \sin^{-1}\left(\frac{\gamma_\perp}{2\gamma_\parallel}\right) \tag{6}$$

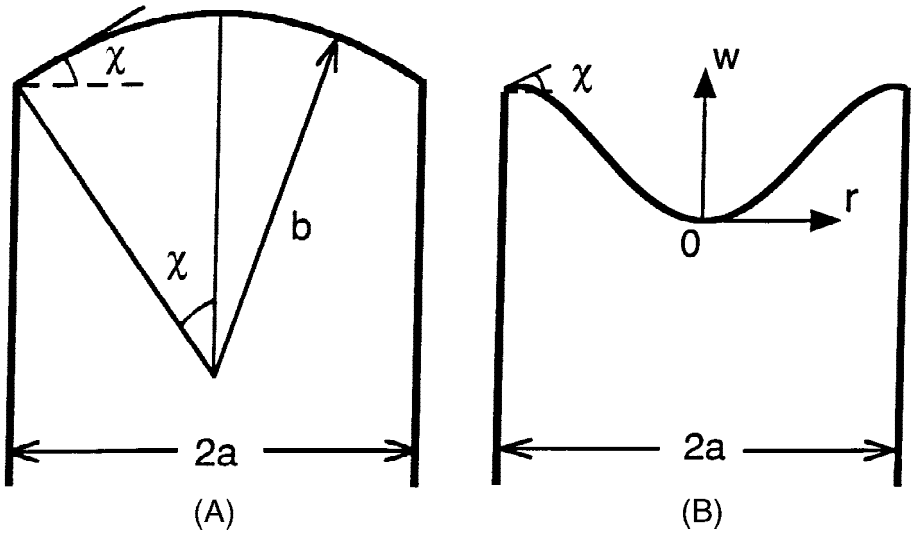

Fig. 2. Cross section of a crystal with cylindrical symmetry and (A) an equilibrium end cap of radius b drawn from the center of curvature and (B) a nonequilibrium end cap of a wavy shape with a profile specified by the coordinates (w,r) (the reference point (0,0) is set at the center of the end cap).

where χ is a thermodynamic quantity that is determined by the ratio of the surface energies. For a cylindrical rod with a relatively low side surface energy, compared to the end surface energy, a small χ is expected.

According to Hwang and Chen,[20,35] the morphology of the hexagonal Si_3N_4 prism can be rationalized in terms of the periodic bond chain (PBC) theory of Hartman.[36] They found from the PBC theory that $\{1\bar{1}00\}$ surfaces should be the flat faces, as are $\{1\bar{1}01\}$ surfaces. The β-Si_3N_4 single crystals grown from a silicon melt or formed via a chemical vapor deposition (CVD) process are indeed enveloped by these faces, which grow along the [0001] direction. The angle between $\{1\bar{1}01\}$ and the (0001) plane is 24°, which corresponds to $\chi = 0.4189$.[35] This value will be used in the example calculations shown below.

(2) Steady-State, Nonequilibrium Shape

During growth, the shape of either the side or the ends may depart from equilibrium. However, continuity of the chemical potential must be observed. The singular nature of the edge also guarantees that the same angle χ at the corner is maintained. As the shape deviates from equilibrium, the local chemical potential may deviate from the equilibrium value. The atomic flux driven by the gradient of the chemical potential alters the shape until a steady state is finally obtained.

We solve the shape of the end cap in the cylindrical coordinates by assuming that surface diffusion is the only transport mechanism and that a steady state can be attained. Attachment of atoms that arrive directly from the liquid is treated as secondary (see discussion at the end of the section). A steady state is defined by a constant axial velocity $V_{||}$ at every point of the end cap. The governing equation obtained from surface diffusion and mass conservation is then

$$\delta_r M_r \nabla_r^2 \mu_r = V_{||} \tag{7}$$

In this equation, ∇_r^2 is the Laplace operator in the radial direction in the cylindrical coordinates, μ_r is the chemical potential at radius r from the center, δ_r is the thickness of the surface diffusion layer at the end caps, and M_r, which is defined as

$$M_r = \frac{D_r}{kT} \tag{8}$$

(where D_r is the surface diffusivity in the radial direction and kT has its usual thermodynamic meaning), is the atomic mobility due to surface diffusion in the radial direction on the end caps. This equation can be solved to determine the shape of the end cap, under appropriate boundary conditions, if we express μ_r in terms of spatial coordinates, using Eq. (1).

To obtain an analytical solution, we linearize Eqs. (1) and (7) in terms of the axial displacement w, with reference to the position at $r = 0$. The linearization procedure is accurate if $w << a$ (which is equivalent to $\chi << 1$); however, it also allows us to obtain some insight even at larger w/a values when its accuracy is less adequate. This procedure gives

$$\kappa_1 = \frac{d^2 w}{dr^2} \tag{9}$$

$$\kappa_2 = \left(\frac{1}{r}\right)\frac{dw}{dr} \tag{10}$$

and

$$V_{||} = \frac{dw}{dt} \tag{11}$$

which transforms Eqs. (1) and (7) to

$$\mu_r = -\Omega\gamma_{||}\nabla_r^2 w \tag{12}$$

and

$$M_r \delta_r \gamma_{||} \Omega \nabla_r^2 \nabla_r^2 w + \frac{dw}{dt} = 0 \tag{13}$$

respectively, where

$$\nabla_r^2 = \frac{d^2}{dr^2} + \left(\frac{1}{r}\right)\frac{d}{dr} \tag{14}$$

The boundary conditions are $w = 0$ at $r = 0$ by definition, $dw/dt = 0$ at $r = 0$ from symmetry, $dw/dt = -\tan\chi \approx \chi$ at $r = a$ within the linearization approximation, and all curvatures are finite and continuous, especially at $r = 0$. The solution to Eq. (13) that satisfies the above-mentioned boundary conditions is

$$\frac{w}{a} = -\left(\frac{S}{4}\right)\left(\frac{r}{a}\right)^4 + \left(\frac{1}{2}\right)(S - \chi)\left(\frac{r}{a}\right)^2 \tag{15}$$

Here, S is a shape parameter that is defined as

$$S = \frac{a^3 V_{||}}{16 M_r \delta_r \gamma_{||} \Omega} \tag{16}$$

The above-mentioned solution is plotted in Fig. 3 for several shape parameters, assuming $\chi = 0.4189$ (i.e., 24°). A convex, spherical cap shape is recovered, within the spirit of linearization approximation, when $S = 0$, giving

$$w = -\left(\frac{\chi}{2a}\right)r^2 \tag{17}$$

As S increases to 2χ, the end cap becomes almost ''flat,'' with $w = 0$ at both $r = 0$ and $r = a$. As S increases further, a severely concave shape develops, except near $r = a$. This shape evolution has been experimentally observed in the (Si,Al,Mg,Y)(O,N) system.

The physical meaning of the shape parameter S can be appreciated from the following consideration. At the steady state, a characteristic time τ_o for axial growth can be defined as

$$\tau_o = \frac{a}{V_{||}} \tag{18}$$

This parameter is the time required to grow a distance comparable to the cylindrical radius. Meanwhile, the relaxation time (τ_r) for surface diffusion along the spherical cap of an arc $2a$ may be expressed as[31]

$$\tau_r = \frac{a^4 kT}{16 D_r \delta_r \gamma_{||} \Omega} = \frac{a^4}{16 M_r \delta_r \gamma_{||} \Omega} \tag{19}$$

It follows that S is simply the ratio of surface relaxation time τ_r to the characteristic growth time τ_o. When this ratio is small, the end cap is fully relaxed by surface diffusion so that an equilibrium, spherical shape is retained. Conversely, when this ratio is large, the end cap severely deviates from the equilibrium shape. A large cylinder radius, a fast growth velocity, and a slow surface diffusivity favor nonequilibrium and a large S value.

(3) Fluxes and Growth Rates

The concave shape of a nonequilibrium end cap implies a surface flux that transports matter from the edge at $r = a$ toward the center at $r = 0$. This influx is responsible for the axial growth. We can compute the surface flux at the edge using the following equation:

$$J_r = -M_r\left(\frac{d\mu_r}{dr}\right) = M_r \gamma_{||} \Omega \left(\frac{d}{dr}\right)(\nabla_r^2 w) \tag{20}$$

giving

$$J^* = \frac{a V_{||}}{2\delta_r} \tag{21}$$

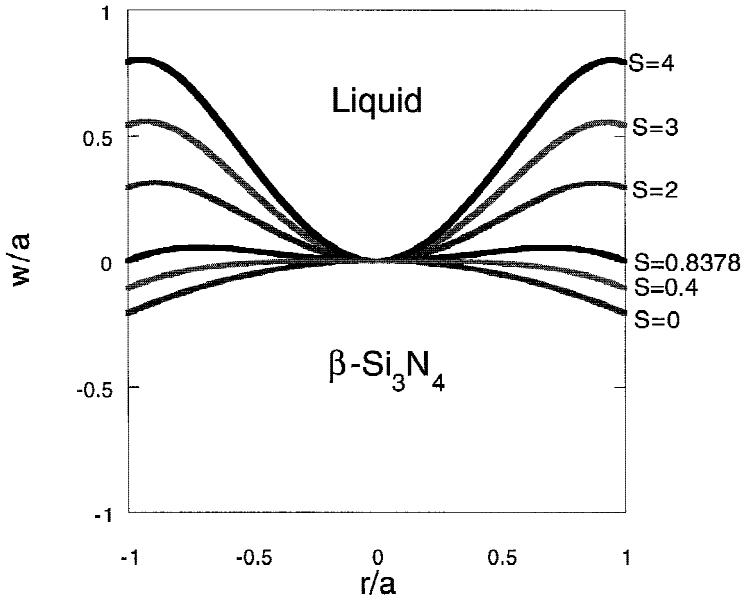

Fig. 3. Predicted steady-state profile of the end of a growing Si_3N_4 crystal. At $S = 0$, a spherical shape is obtained. At $S = 2\chi = 0.8378$, $w = 0$ at $r = a$; the angle at $r = a$ is fixed at 24° ($\chi = 0.4189$).

at $r = a$. In Eq. (21), the subscript for J^* has been omitted for simplicity. This result can be easily verified, because the rate of total mass accumulation on the end cap, $\pi a^2 V_{\|}$, must be supplied by J^* at the edge over a conduit of an area $2\pi a\delta_r$. Thus, a fast growth rate requires a large surface flux at the edge.

The magnitude of the surface flux passing the circular edge at $r = a$ also determines the shape of the end caps. For a given radius a, S can be rewritten as

$$S = \frac{a^2 J^*}{8M_r\gamma_{\|}\Omega} = \frac{a^2 J^* kT}{8D_r\gamma_{\|}\Omega} \tag{22}$$

Thus, a large influx, a large cylindrical radius, and a small surface diffusivity on the end surface lead to a nonequilibrium shape.

A nonequilibrium shape of the end cap also implies a nonequilibrium edge potential at $r = a$. The value can be computed from Eq. (12), which gives

$$\mu^* = (\chi + S)\left(\frac{2\gamma_{\|}\Omega}{a}\right) \tag{23}$$

at $r = a$. (The subscript r of μ^* has again been omitted for simplicity.) At equilibrium, $S = 0$ and $\mu^* = 2\gamma_{\|}\Omega\chi/a$, which reduces to Eq. (3) within the spirit of linearization. For a nonequilibrium shape, the chemical potential at $r = a$ is higher than that of the equilibrium shape by a factor of S/χ; the larger the shape factor, the higher the edge potential.

Using the edge potential, we can further obtain the upper and lower limits of S and $V_{\|}$ from the following consideration. For a cylindrical rod embedded in a field of supersaturation, the maximum value of μ^* is simply μ^∞, which is the chemical potential at a far distance from the cylinder. From this observation, we obtain the upper limit of S ($S^{\max}$), using Eq. (23):

$$S^{\max} = \left(\frac{\mu^\infty}{\mu^\circ} - 1\right)\chi \tag{24}$$

where the equilibrium surface chemical potential μ° is defined by

$$\mu^\circ = \frac{\gamma_{\perp}\Omega}{a} = \frac{2\gamma_{\|}\Omega}{b} \tag{25}$$

This relation also sets the upper limit of the surface flux—and, hence, the axial velocity ($V_{\|}^{\max}$)—through Eqs. (21), (22), and (24):

$$V_{\|}^{\max} = \frac{8M_r\delta_r(\mu^\infty - \mu^\circ)}{a^2} \tag{26}$$

This maximum velocity is only dependent on the surface diffusivity at the end cap, because all of the driving force, $\mu^\infty - \mu^\circ$, is dissipated there. Conversely, the lower limit of μ^* is μ° and the lower limit of S is zero. The lower limit of growth velocity, at $S = 0$, however, does not originate from surface diffusion, because when the equilibrium shape is attained, there is no gradient in the surface chemical potential and, hence, no flux. In this case, the other growth mode, namely atoms arriving directly from the liquid to the end caps, becomes important. This case is treated as a problem of steady-state diffusion toward a spherical sink of radius b, which is a standard problem in diffusion and gives a growth rate[37]

$$V_{\|}^{\circ} = \frac{M_\ell(\mu^\infty - \mu^\circ)}{b - \dfrac{b^2}{R}} \tag{27}$$

Here, M_ℓ is the atomic mobility in the liquid and R is the radius of the influence sphere around a rod, which may be assumed to be the half spacing between rods. For $R >> b$ and substituting a/χ for b, we obtain the growth rate of an equilibriated end cap:

$$V_{\|}^{\circ} = \frac{M_\ell\chi(\mu^\infty - \mu^\circ)}{a} \tag{28}$$

More generally, for end caps of nonequilibrium shapes, we may obtain the approximate total growth rate by adding $V_{\|}^{\circ}$ to any $V_{\|}$ due to surface flux. Here, we have assumed that liquid diffusion does not alter the surface shape; that is, atoms that are transported to the end cap by surface diffusion do not redissolve into the liquid and redeposit elsewhere.

III. Effect of Supersaturation, Aspect Ratio, and Liquid/Surface Mobilities

The solution in Section II clearly indicates the importance of the surface flux J^* at the edge. This flux originates from atoms

collected on the side surface of the cylinder, which are poured into the end caps by surface diffusion. Qualitatively, we expect J^* to increase as the supersaturation increases in the liquid from which the initial atoms originate. We also expect J^* to increase, up to a certain limit, as the length of the cylinder that determines the collection distance increases. A more-precise determination of J^*, by solving the appropriate diffusion equations in the liquid and on the side surface, is made below, again for the steady state.

We assume that the chemical potential on the side surface varies with the axial coordinate z, from $\mu_z = \mu^*$ at the end ($z = L$) to higher values toward the mid-section of the cylinder ($z = 0$). The difference between μ^∞ and μ_z causes atomic transport in the liquid toward the cylinder, and the difference between μ_z and μ^* causes atomic transport by surface diffusion along the side surface toward the end caps. For simplicity, we allow no radial growth on the side surface. This condition is equivalent to the assumption that there is a threshold value of μ_z that must be exceeded on the side surface before radial growth occurs, and that the driving force available is insufficient to overcome this threshold.[38] (In other words, we assume that the side surface may accept adsorbed atoms, but the adsorbed atoms are not permanently attached to the side surface. Rather, they are constantly transported away by surface diffusion.) Then, conservation of mass demands

$$\delta_z M_z \frac{d^2\mu_z}{dz^2} = -J_{\ell z} \tag{29}$$

Here, M_z is the atomic mobility due to surface diffusion along the ***z***-axis, δ_z the thickness of surface diffusion layer on the side surface, and $J_{\ell z}$ the atomic flux from liquid arriving at the side surface at the position z.

We will not solve $J_{\ell z}$ in the general case of z-varying μ_z. Instead, we will use the solution of steady-state diffusion toward an infinitely long cylindrical sink of a constant surface potential. This surface potential is taken as μ_z. The problem is then reduced to a standard one in diffusion and has the following solution:[37]

$$J_{\ell z} = \frac{M_\ell(\mu^\infty - \mu_z)}{a \ln\left(\frac{R}{a}\right)} \tag{30}$$

Substituting Eq. (30) into Eq. (29), we obtain

$$\frac{d^2(\mu_z - \mu^\infty)}{dz^2} = \left[\frac{M_\ell}{M_z\delta_z a \ln\left(\frac{R}{a}\right)}\right](\mu_z - \mu^\infty) \tag{31}$$

with the boundary condition of $\mu_z = \mu^*$ at $z = \pm L$. Equation (31) is the governing equation for diffusion on the side surface.

The solution of Eq. (32) that satisfies the boundary condition is

$$\frac{\mu_z - \mu^\infty}{\mu^* - \mu^\infty} = \frac{\cosh\left[\frac{M_\ell z^2}{M_z\delta_z a \ln\left(\frac{R}{a}\right)}\right]^{1/2}}{\cosh\left[\frac{M_\ell L^2}{M_z\delta_z a \ln\left(\frac{R}{a}\right)}\right]^{1/2}} \tag{32}$$

Thus, the surface potential has now been determined within a constant μ^* value. This constant is not an independent one: it is related to the surface flux J^* at the edge through Eqs. (22) and (23). The surface flux J^* can be obtained by either integrating J_ℓ over the half length, $z = 0$ to L, or by directly evaluating $M_z(d\mu_z/dz)$ at $z = L$. These two methods, of course, give the same result. (Here, we need to include a factor δ_z/δ_r to convert the surface flux on the side surface to that on the end cap.)

$$J^* = (\mu^\infty - \mu^*)\left[\frac{\delta_z M_z M_\ell}{\delta_r^2 a \ln\left(\frac{R}{a}\right)}\right]^{1/2} \times \tanh\left[\frac{M_\ell L^2}{M_z\delta_z a \ln\left(\frac{R}{a}\right)}\right]^{1/2} \tag{33}$$

Rewriting J^* in terms of the axial velocity of the end caps (Eq. (21)), we obtain

$$V_\parallel = 2\left(\frac{\mu^\infty - \mu^*}{a}\right) \times \left[\frac{\delta_z M_z M_\ell}{a \ln\left(\frac{R}{a}\right)}\right]^{1/2} \tanh\left[\frac{M_\ell L^2}{M_z\delta_z a \ln\left(\frac{R}{a}\right)}\right]^{1/2} \tag{34}$$

Also rewriting μ^* in terms of $V_\parallel$, using Eqs. (23) and (16), we obtain

$$\mu^* - \mu^\infty = \mu^\circ - \mu^\infty + \frac{a^2 V_\parallel}{8 M_r \delta_r} \tag{35}$$

Eliminating the term $\mu^\infty - \mu^*$ from Eqs. (34) and (35) in favor of $V_\parallel$, we obtain

$$V_\parallel = \left(\frac{\mu^\infty - \mu^\circ}{a}\right)\left\{2\left[\frac{\delta_z M_z M_\ell}{a \ln\left(\frac{R}{a}\right)}\right]^{1/2} \tanh\left[\frac{M_\ell L^2}{M_z\delta_z a \ln\left(\frac{R}{a}\right)}\right]^{1/2}\right\} \times \left\{1 + \frac{1}{4}\left[\frac{a\delta_z M_z M_\ell}{\delta_r^2 M_r^2 \ln\left(\frac{R}{a}\right)}\right]^{1/2} \tanh\left[\frac{M_\ell L^2}{M_z\delta_z a \ln\left(\frac{R}{a}\right)}\right]^{1/2}\right\}^{-1} \tag{36}$$

Thus, the axial growth velocity $V_\parallel$ is entirely determined by the difference between the supersaturation in the far field (μ^∞) and the equilibrium chemical potential of a rod (μ°). Only the kinetics are dependent on geometry (a, L, and R) and mobilities M_ℓ, M_z, and M_r. Using Eq. (35) again, we obtain

$$\mu^* = \mu^\circ + \frac{a^2 V_\parallel}{8 M_r \delta_r} = \mu^\circ + (\mu^\infty - \mu^\circ)\left\{\frac{1}{4}\left[\frac{a\delta_z M_z M_\ell}{\delta_r^2 M_r^2 \ln\left(\frac{R}{a}\right)}\right]^{1/2} \tanh\left[\frac{M_\ell L^2}{M_z\delta_z a \ln\left(\frac{R}{a}\right)}\right]^{1/2}\right\} \times \left\{1 + \frac{1}{4}\left[\frac{a\delta_z M_z M_\ell}{\delta_r^2 M_r^2 \ln\left(\frac{R}{a}\right)}\right]^{1/2} \tanh\left[\frac{M_\ell L^2}{M_z\delta_z a \ln\left(\frac{R}{a}\right)}\right]^{1/2}\right\}^{-1} \tag{37}$$

Therefore, the chemical potential at the edge is also dependent on the quantity $\mu^\infty - \mu^\circ$ and the same sets of geometric and mobility parameters. Lastly, from Eqs. (16) and (36), we obtain

$$S = \chi\left(\frac{\mu^\infty}{\mu^\circ} - 1\right)\left\{\frac{1}{4}\left[\frac{a\delta_z M_z M_\ell}{\delta_r^2 M_r^2 \ln\left(\frac{R}{a}\right)}\right]^{1/2} \tanh\left[\frac{M_\ell L^2}{M_z\delta_z a \ln\left(\frac{R}{a}\right)}\right]^{1/2}\right\} \times \left\{1 + \frac{1}{4}\left[\frac{a\delta_z M_z M_\ell}{\delta_r^2 M_r^2 \ln\left(\frac{R}{a}\right)}\right]^{1/2} \tanh\left[\frac{M_\ell L^2}{M_z\delta_z a \ln\left(\frac{R}{a}\right)}\right]^{1/2}\right\}^{-1} \tag{38}$$

from which we can determine the shape of the end cap. The solution of the steady-state problem is now complete.

IV. Limiting Cases for Kinetic Control and Shape Transition

We have already obtained two limiting solutions in Section II(*3*) by setting μ^* as either μ^∞ or μ°. This determination, in

turn, leads to S^{max} and $V_{\|}^{max}$ or $S = 0$ and $V_{\|}^{\circ}$ as the limiting solution. These two limits are absolute ones, which respectively correspond to the maximum deviation from the equilibrium shape and the equilibrium shape itself, and they are independent of the length of the cylinder, the kinetics of surface diffusion on the side, and the atomic mobility in the liquid. However, the latter factors are expected to lead to intermediate solutions that are applicable in intermediate cases of kinetics and aspect ratio. This expectation is explored below.

The limiting cases are examined by referring to the shape parameter. To simplify the discussion, we introduce the following parameters:

$$\alpha_\ell = \frac{M_\ell L}{a \ln\left(\frac{R}{a}\right)} \tag{39}$$

$$\alpha_z = \frac{M_z \delta_z}{L} \tag{40}$$

$$\alpha_r = \frac{M_r \delta_r}{a} \tag{41}$$

These parameters have the physical meaning of ''conductance,'' because they are proportional to the mobility and the cross section of each pathway and are inversely proportional to the effective diffusion distance along the respective pathway. In terms of these parameters, the shape parameter S (Eq. (38)) can be recast as

$$S = \chi\left(\frac{\mu^{\infty}}{\mu^{\circ}} - 1\right)\left[\frac{\frac{1}{4}\left(\frac{\alpha_\ell \alpha_z}{\alpha_r^2}\right)^{1/2} \tanh\left(\frac{\alpha_\ell}{\alpha_z}\right)^{1/2}}{1 + \frac{1}{4}\left(\frac{\alpha_\ell \alpha_z}{\alpha_r^2}\right)^{1/2} \tanh\left(\frac{\alpha_\ell}{\alpha_z}\right)^{1/2}}\right] \tag{42}$$

Three limiting cases can now be differentiated.

(1) Case (i): ¼$(\alpha_\ell \alpha_z/\alpha_r^2)^{1/2}$ tanh $(\alpha_\ell/\alpha_z)^{1/2} >> 1$

With $S = \chi[(\mu^{\infty} - \mu^{\circ}) - 1]$, this reduces to the case of $\mu^* = \mu^{\infty}$ and $V_{\|}^{max}$. The kinetics are entirely controlled by surface diffusion on the end cap and are independent of the aspect ratio and kinetics elsewhere. The shape is at the maximum deviation from the equilibrium.

(2) Case (ii): ¼$(\alpha_\ell \alpha_z/\alpha_r^2)^{1/2}$ tanh $(\alpha_\ell/\alpha_z)^{1/2} << 1$ and $\alpha_\ell/\alpha_z << 1$

Under these conditions, S becomes

$$S = \frac{1}{4}\left(\frac{\alpha_\ell}{\alpha_r}\right)\chi\left(\frac{\mu^{\infty}}{\mu^{\circ}} - 1\right) \tag{43}$$

It follows that $S << 1$. Thus, a quasi-equilibrium shape is maintained, which implies $\mu^* \approx \mu^{\circ}$. The axial growth rate can be obtained from Eq. (36), which is reduced to

$$V_{\|} = 2\left(\frac{L}{a}\right)\frac{M_\ell(\mu^{\infty} - \mu^{\circ})}{a \ln\left(\frac{R}{a}\right)} \tag{44}$$

That is, it is entirely controlled by α_ℓ.

Comparing Eq. (44) (quasi-equilibrium growth) with Eq. (28) (equilibrium growth) ($S = 0$ and $\mu^* = \mu^{\circ}$), we see that the axial growth rate is similarly controlled by M_ℓ but is also enhanced by an aspect ratio $2(L/a)$. This result can be easily verified from the consideration of mass conservation. The total rate of incoming material from the side is $2\pi a L M_\ell (\mu^{\infty} - \mu^{\circ})/[a \ln (R/a)]$ by setting $\mu_z = \mu^{\circ}$ in Eq. (30). The total growth rate of material on the cap is $\pi a^2 V_{\|}$. Thus, $V_{\|}$ of Eq. (44) results.

The present case applies when the liquid conductance is much smaller than either surface conductance. This observation is evident from the above-discussed consideration ($\alpha_\ell/\alpha_z << 1$ and $\alpha_\ell/\alpha_r << 1$ by combining the two inequalities of case (ii)). The side surface acts as a collector that enhances the axial growth rate. The total growth rate, considering the side contribution (Eq. (44)) and the end-cap contribution (Eq. (28)), is

$$V_{\|}^{total} = 2\left(\frac{L}{a} + 1\right)\frac{M_\ell(\mu^{\infty} - \mu^{\circ})}{a \ln\left(\frac{R}{a}\right)} \tag{45}$$

(3) Case (iii): ¼$(\alpha_\ell \alpha_z/\alpha_r^2)^{1/2}$ tanh $(\alpha_\ell/\alpha_z)^{1/2} << 1$ and $\alpha_\ell/\alpha_z >> 1$

The shape factor S becomes

$$S = \frac{1}{4}\left(\frac{\alpha_\ell \alpha_z}{\alpha_r^2}\right)^{1/2}\chi\left(\frac{\mu^{\infty}}{\mu^{\circ}} - 1\right) \tag{46}$$

By combining the two inequalities of case (iii), we obtain ¼$(\alpha_\ell \alpha_z/\alpha_r^2)^{1/2} << 1$. It follows that $S << 1$. Thus, a quasi-equilibrium shape is again maintained, which implies $\mu^* \approx \mu^{\circ}$. The axial growth rate is obtained from Eq. (36) in the appropriate limit:

$$V_{\|} = 2\left(\frac{\alpha_\ell}{\alpha_z}\right)^{1/2}\left(\frac{\mu^{\infty} - \mu^{\circ}}{a}\right) = 2\left[\frac{\delta_z M_z M_\ell}{a \ln\left(\frac{R}{a}\right)}\right]^{1/2}\left(\frac{\mu^{\infty} - \mu^{\circ}}{a}\right) \tag{47}$$

It is controlled by the geometric mean of the conductance of the liquid and the side surface but is independent of the length of the cylinder. Thus, it is obviously an intermediate case between cases (i) and (ii), despite the quasi-equilibrium shape being similar to that of case (ii).

The reason for the length independence in this case can be found from the condition $\alpha_\ell/\alpha_z >> 1$ of case (iii). Using the definitions of α_ℓ and α_z, we find the condition to be equivalent to

$$L >> \left[\left(\frac{M_z}{M_\ell}\right)\delta_z a \ln\left(\frac{R}{a}\right)\right]^{1/2} \equiv L^* \tag{48}$$

Thus, as the cylinder becomes longer than a certain length L^*, only side surface diffusion near the end cap within a distance L^* becomes relevant. Beyond that, $\mu_z \approx \mu^{\infty}$, because of the relatively high ratio of α_ℓ/α_z. (Mathematically, this is manifested by $\tanh x = 1$ when $x >> 1$.) This is equivalent to stating that the efficiency of the side surface acting as a collector diminishes as the length increases when the liquid conductance is high relative to the surface conductance. This situation must be the case; otherwise, an infinitely long cylinder would have collected an infinite mass to be poured into the end caps.

In summary, we can restate the above-discussed three cases as follows. When the liquid conductance is the smallest, as given by case (ii), the side surface acts as an efficient collector and the axial velocity is enhanced by a factor of $2(L/a)$ over the (liquid) diffusion-controlled solution of a spherical cap. The shape of the end cap is almost an equilibrium one. As the liquid conductance becomes larger than the side surface conductance, as given by case (iii), the side surface acts as an inefficient collector and the axial velocity is controlled by the geometric mean of the atomic mobilities in the liquid and on the side surface but is independent of the length L. The shape of the end cap is still almost an equilibrium one; this condition is case (iii). When the combination of liquid conductance and the side surface conductance is high, compared to the end surface conductance, as given by case (i), the side surface and the edge have a potential that is equal to the supersaturation, i.e., $\mu_z = \mu^* = \mu^{\infty}$, and the shape reaches the maximum deviation from equilibrium. The kinetics are entirely controlled by surface diffusion on the end cap and are independent of the aspect ratio and the kinetics elsewhere.

Generally, the last case (case (i)) can be satisfied if the following condition is met:

$$\frac{\alpha_\ell \alpha_z}{\alpha_r^2} >> 1 \tag{49}$$

which is equivalent to

$$\frac{\left(\frac{M_\ell M_z}{M_r^2}\right)\left(\frac{a\delta_z}{\delta_r^2}\right)}{\ln\left(\frac{R}{a}\right)} >> 1 \tag{50}$$

Then, this is the condition for the shape transition and highly nonequilibrium growth. Conversely, when the inequality of Eq. (50) is reversed, quasi-equilibrium shape and growth are achieved, although two subcases can be further differentiated, depending on whether or not $L > L^*$ (Eq. (48)).

The above-discussed three cases can also be illustrated by the profile of chemical potential on the side surface; this profile is schematically shown in Fig. 4. In case (i), the potential on the side surface is the same as μ^∞. In case (ii), the potential on the side surface is very similar to $\mu°$, although the exact magnitude is dependent on M_z. The chemical potential in the intermediate case (case (iii)) increases from $\mu°$ at the end to μ^∞ within a distance on the order of L^*, which is dependent on M_z.

V. Discussion

(1) Shape Evolution

The analysis of the previous section suggests three cases of interest for the growth of well-separated crystals: quasi-equilibrium with liquid control, quasi-equilibrium with mixed control, and nonequilibrium with surface control. For growth conditions in a liquid that contains a small amount of solid, we believe the second and the third cases will be very easy to realize. The condition of quasi-equilibrium with mixed control is given by Eq. (48), which is equivalent to an aspect ratio $L/a >> [(M_z M_\ell)(\delta_z/a) \ln (R/a)]^{1/2}$. Typically, δ_z is on the order of a unit-cell dimension and a is on the order of 1 μm, so $\delta_z << a$. Because we expect M_z to be smaller than M_ℓ and $\ln (R/a)$ is of the order of unity, the right-hand side of the above-mentioned inequality is probably <1 and the condition is readily satisfied. Therefore, we can state that the growth of well-isolated Si_3N_4 crystals is at least partially controlled by surface diffusion, even in the quasi-equilibrium case. The condition of nonequilibrium growth is given by Eq. (50). Because we expect liquid diffusion to be at least as fast as surface diffusion, $(M_\ell M_z)^{1/2}$ is probably on the same order as M_r. Meanwhile, $a >> \delta_z \approx \delta_r$, and again $\ln (R/a) \approx 1$, so Eq. (48) should also be readily satisfied. This observation means the growth of isolated Si_3N_4 crystals is probably controlled by surface diffusion on the end cap, and the shape is simply determined by the ratio of supersaturation to $\mu°$ through Eq. (24).

The above prediction suggests that, essentially from the very beginning, the nonequilibrium form has manifested itself. However, the shape parameter S, which is equal to $[(\mu^\infty/\mu°) - 1]\chi$, is dependent on size. When a critical nucleus forms, the size of the critical nucleus, a^*, is given by the relation $a^* = \gamma_\perp \Omega/\mu^\infty$.[39] Thus, $\mu^\infty/\mu° = 1$ and $S = 0$. As the crystal grows larger, $\mu°$ (which is equal to $\gamma_\perp \Omega/a$) decreases, so that the value of S increases. In reality, the supersaturation probably also decreases after nucleation begins. However, to provide the driving force for growth, it is clear that $\mu^\infty/\mu°$ must be >1, and it probably continues to increase for at least some time during the growth stage. Eventually, as the concentration of excess atoms is depleted, the source of supersaturation changes to that provided by the dissolution of the smaller crystals. This supersaturation continues to feed the large crystals in what is known as the Oswald ripening process.[40] During this process, the ratio $\mu^\infty/\mu°$ is determined by $\mu°(a_1)/\mu°(a_2) = a_2/a_1$, where a_1 and a_2 are the radii of the (smaller) dissolving crystal and the (larger) growing crystal, respectively.

In summary, we suggest that the shapes observed in the growth of isolated grains represent a spectrum of shape evolution controlled by $\mu^\infty/\mu°$. This is illustrated schematically in Fig. 5 by the evolution of μ^∞, $\mu°$, $\mu^\infty/\mu°$, and S during the stages of nucleation, growth, and coarsening. We suggest that, after nucleation, although μ^∞ and $\mu°$ both decrease monotonically, their ratio increases as the radius of the crystal increases. As the growth stage passes and the coarsening stage begins, the value of $\mu^\infty/\mu°$ becomes the ratio of the crystal size and is determined by the size dispersity of the crystal population. Therefore, highly nonequilibrium shapes can be observed in two cases: (i) in the growth stage when the crystals are large, and (ii) in the coarsening stage when the polydispersity is large. This prediction is consistent with the experimental observations.[25] For example, large shape distortions of Si_3N_4 have been observed in three liquid systems ((Si,Al,Mg)(O,N), (Si,Al,Y)(O,N), and (Si,Al,Mg,Y)(O,N)) when the crystals are

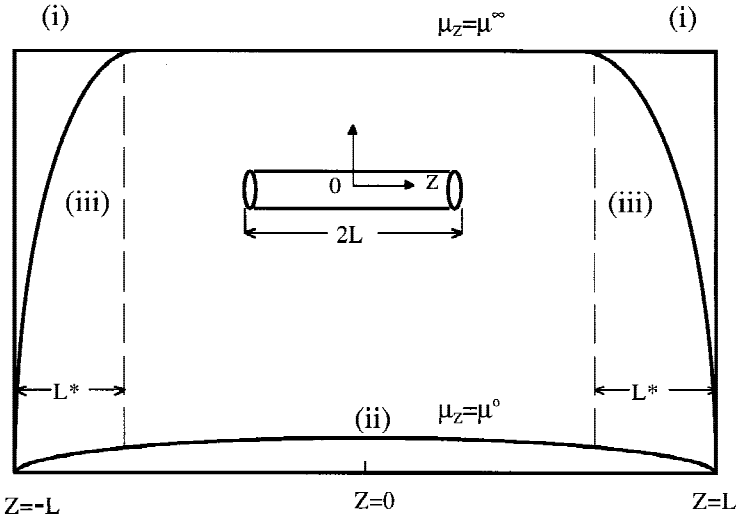

Fig. 4. Schematic distribution of the chemical potential on the side surface of a cylindrical rod of a length 2*L* (see inset). In case (i), liquid diffusion is very fast and the chemical potential on the side surface is the same as supersaturation. In case (ii), liquid diffusion is very slow and the chemical potential is approximately $\mu°$ but is slightly higher, following a parabolic curve centered at $Z = 0$. Case (iii) shows an intermediate case, with the chemical potential increasing from $\mu°$ to μ^∞ within a distance L^* from either end.

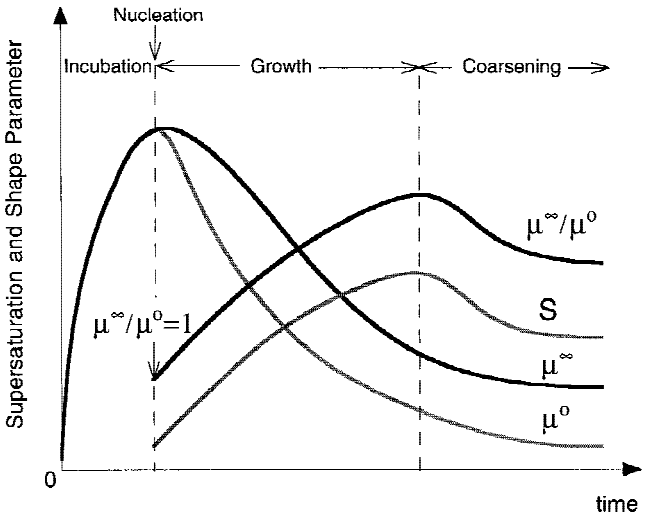

Fig. 5. Schematic evolution of supersaturation (μ^∞) and the shape factor (S) during the nucleation, growth, and coarsening stages of Si_3N_4 in a melt. Also shown are equilibrium chemical potentials of the crystal (μ°) and the ratio of μ^∞ to μ°.

large. Furthermore, among the three systems, the polydispersity is the largest in the (Si,Al,Mg,Y)(O,N) system, where the most-severe shape distortion is observed. Lastly, in the (Si,Al,Y)(O,N) system, the crystals are smaller but more numerous, and the polydispersity is also the smallest. As expected from our analysis, the shape distortion is relatively modest in the (Si,Al,Y)(O,N) system.

(2) Radial Growth

As we mentioned in the introduction, direct influx from the liquid to the end cap will have a tendency to smooth out the shape distortion to restore the equilibrium shape. Surface diffusion would have the same effect if the influx were not to originate only from the edge. However, if the influx does originate from the edge, then a shape distortion with a convex edge and a concave center must be maintained to distribute the matter from the edge to the center. Because an isolated crystal with an atomically flat surface readily receives liquid flux from the side but is unable to accommodate the influx atoms permanently onto the surface structure on the side, this influx is directed to the edge and then the end cap, where the surface structure is atomically rough and more accommodating. As the aspect ratio becomes large, this becomes the dominant mechanism for axial growth and is responsible for the nonequilibrium shape distortion of the end caps.

The importance of the above-mentioned mechanism diminishes if the side surface can accommodate the atomic influx, i.e., if it grows radially. For an isolated crystal growing in a liquid environment, our analysis in Sections II–IV can be readily modified to account for radial growth. We assume that the radial growth has a velocity $V_\perp$ that is not dependent on the axial coordinate z. Then, Eq. (29) is modified to become

$$(\delta_z M_z)\frac{d^2\mu_z}{dz^2} = -J_\ell + V_\perp \tag{51}$$

Because $V_\perp$ is independent of z, $V_\perp$ can be absorbed into the flux term J_ℓ by regarding it as an effective potential, using Eq. (30). Specifically, by substituting Eq. (30) into Eq. (51) and changing the variable, we obtain a modified form of Eq. (31) in which μ^∞ is replaced by $\tilde{\mu}^\infty$ (the effective supersaturation). This supersaturation is defined as follows:

$$\tilde{\mu}^\infty = \mu^\infty - \left(\frac{aV_\perp}{M_\ell}\right)\ln\left(\frac{R}{a}\right) \tag{52}$$

With the definition of $\tilde{\mu}^\infty$, we then find that all the solutions of μ_z, μ^*, S, and $V_\parallel$ in Sections II–IV are recovered if we simply substitute $\tilde{\mu}^\infty$ for μ^∞, because the only effect of radial growth is to take away a portion of the liquid influx, which is equivalent to a decrease of the supersaturation. Since the conditions for the kinetic and shape transitions (given in Section IV) are all independent of the driving force, the radial growth has no effect on the transitions. In this sense, we have found justification to ''decouple'' the radial growth problem from the shape transition problem. However, we recognize that the radial growth does reduce μ^*, S, and $V_\parallel$, because $\tilde{\mu}^\infty$ is smaller than μ^∞, according to Eq. (52).

The above-mentioned effect is important if the ''effective kinetic'' potential ($(aV_\perp/M_\ell)\ln(R/a)$) is large, in comparison to $\mu^\infty - \mu^\circ$. This result is not expected to be the case for the growth of isolated Si_3N_4 crystals. For example, using Eq. (26), we find that the ratio of the quantity $\mu^\infty - \mu^\circ$ to the kinetic potential is given by

$$\frac{\mu^\infty - \mu^\circ}{\mu^\infty - \tilde{\mu}^\infty} = \frac{\left(\frac{a}{\delta_r}\right)\left(\frac{M_\ell}{M_r}\right)\left(\frac{V_\parallel}{V_\perp}\right)}{\ln\left(\frac{R}{a}\right)} \tag{53}$$

This ratio is probably quite large, given the typical anisotropy in the growth rate ($V_\parallel/V_\perp \approx 10$ in most experiments[18,21–25]) and the fact that $a/\delta_r > 100$, $M_\ell > M_r$ (in most cases), and $\ln(R/a) \approx 1$. Therefore, the omission of the radial growth in the analysis of Sections II–IV is not a serious problem and all our conclusions, especially those regarding nonequilibrium growth, should remain valid, even if radial growth is allowed.

The assumption that radial growth is independent of z is tantamount to the assumption of interface control. Under interface control, the velocity is dependent on the potential but is independent of diffusivity in the liquid or along the surface. However, the functional form of the velocity dependence on the surface potential is not known *a priori*. Therefore, we will not attempt to obtain a solution for $V_\perp$ in the case of nonequilibrium growth, considering the lack of importance of radial growth, as reasoned previously.

(3) Silicon Nitride Ceramics

The other situation in which the surface diffusion mechanism and the nonequilibrium shape may become unimportant is when the liquid transport to the side surface is blocked. Without the large influx from the side surface, only direct liquid diffusion to the end cap is significant and the shape distortion disappears. This phenomenon will occur, to an increasing degree, when the solid fraction increases. In a typical silicon nitride ceramic that contains 90% solid grains, the crystals are often stacked so that their side surfaces are in close contact with neighboring crystals, separated by a thin liquid film,[14,41,42] and only the ends are exposed to the liquid pockets. Such a geometry makes it difficult to obtain a substantial influx to the edge. Therefore, Si_3N_4 crystals in high-volume-fraction-solids ceramics are not likely to develop nonequilibrium shapes, except perhaps in the early stages of growth. For such ceramics, several studies have reported a cubic growth law for the length (i.e., $L^3 = L_\circ^3 + k_\parallel t$,[18,21,22] and a higher exponent for the width (e.g., $a^5 = a_\circ^5 + k_\perp t$[22]). (Here, $L_\circ$ and $a_\circ$ respectively refer to the length and radius at the reference time, and t is the time elapsed since the reference time. The rate constants, of an appropriate unit, are represented by the variables k.) In the following, we will assume an equilibrium shape and show that these growth laws can be rationalized.

For equilibrium shape, the chemical potential is μ° everywhere on the crystal surface. For axial growth, we refer to Eq. (28), which is the standard form of diffusive growth of a spherical particle.[37] Assuming $a \propto L$ for the moment (or at least

the aspect ratio is a slow-varying function of the size) and the growth is an Oswald ripening process driven by size differentials, we find the problem reduced to that of particle coarsening.[39] The standard mean field theory then predicts a cubic growth law,[39,43,44] which is consistent with the experimental observation of length growth. For the radial growth, we assume it is interface controlled and is dependent on the potential only. Therefore, we can let

$$V_{\perp} = \frac{da}{dt} = k_{\perp}(\mu^{\infty} - \mu^{\circ})^{n} \tag{54}$$

where $k_{\perp}$ is a rate constant and n is a fitting parameter. Using $\mu^{\circ} = \gamma_{\perp}\Omega/a$ and $\mu^{\infty} = \gamma_{\perp}\Omega/a_1$ (where a_1 is the radii of the dissolving crystals), we find that the above-mentioned kinetics yield, in the mean field theory, the observed radial growth law if $n = 4$. Such a large n value means that the growth rate is very slow at low surface potentials and increases more rapidly at large surface potentials. This observation is consistent with the common notion of interface control.[38,45]

From this discussion, it seems plausible that, in silicon nitride ceramics that contain a small amount of liquid, the growth at the ends of the crystal is diffusion controlled but the growth of the side is interface controlled. As the amount of the liquid increases, however, the side surface becomes more exposed to the liquid; therefore, more diffusional fluxes can be funneled through the side surfaces to the ends, which causes the growth rate of the ends to increase with the amount of liquid. Such an observation has been made in the literature (for example, see Lee *et al.*[19]), although it was used as evidence against diffusion control by arguing that the diffusion distance increases as the amount of liquid increases.[19] As we have shown here, such an argument may not be justified, considering the new growth mechanism that has been discovered in this work.

VI. Conclusions

(1) A new growth mechanism for Si_3N_4 crystals in a liquid environment has been observed. The mechanism allows atom diffusion via the liquid to the side surface, and it further demands that the majority of these atoms be transported to the end caps, to feed axial growth. For large-radius crystals, the redistribution of atoms on the end caps requires a long relaxation time. As a result, a nonequilibrium shape develops there.

(2) A shape parameter has been determined that can be used to describe the shape of the end caps. This parameter is strongly dependent on size, reflecting the requirement of shape relaxation by surface diffusion. It is also dependent on the ratio of the chemical potential at a far distance from the cylinder to the equilibrium surface chemical potential (μ^{∞}/μ°). Large distortion is predicted to occur during the growth stage, if the crystal size is large, and during the Oswald ripening stage, if the size polydispersity is large.

(3) For an isolated Si_3N_4 crystal growing in a liquid environment, neither direct liquid diffusion to the end cap nor the radial growth should be a significant factor that enters the nonequilibrium shape consideration of the end caps.

(4) For a silicon nitride ceramic with a small volume fraction of liquid, the diffusion flux to the side surface is blocked and the above-mentioned mechanism ceases to operate. Shape distortion should not occur, and the equilibrium shape should be obtained. The axial growth in the later stage is via Oswald ripening that is controlled by liquid diffusion. The radial growth is interface controlled and is dependent only on the surface chemical potential.

References

[1]F. F. Lange, ''Relations between Strength, Fracture Energy, and Microstructure of Hot Pressed Si_3N_4,'' *J. Am. Ceram. Soc.*, **56** [10] 518–22 (1973).

[2]E. Tani, S. Umebayashi, K. K. Kikobayashi, and M. Nishijima, ''Gas Pressure Sintering of Si_3N_4 with Concurrent Additives of Al_2O_3 and 5 wt% Rare Earth Oxide: High Fracture Toughness Si_3N_4 with Fiber-like Structure,'' *Am. Ceram. Soc. Bull.*, **65** [9] 1311–15 (1986).

[3]P. F. Becher, H. T. Lin, S.-L. Hwang, M. Hoffman, and I-W. Chen, ''The Influence of Microstructure on the Mechanical Behavior of Silicon Nitride Ceramics''; pp. 147–58 in *Silicon Nitride Ceramics, Scientific and Technological Advances*, Materials Research Society Symposium Proceedings, Vol. 287. Edited by I-W. Chen, P. F. Becher, M. Mitomo, G. Petzow, and T.-S. Yen. Materials Research Society, Pittsburgh, PA, 1993.

[4]G. G. Deeley, J. M. Herbert, and N. C. Moore, ''Dense Silicon Nitride,'' *Powder Metall.*, **8**, 145–51 (1961).

[5]K. Komeya and H. Inoue, ''Heat Resistant Strengthened Composites,'' Jpn. Pat. No. 703695, 1969.

[6]G. R. Terwilliger and F. F. Lange, ''Hot Pressing Behavior of Si_3N_4,'' *J. Am. Ceram. Soc.*, **57** [1] 25–29 (1974).

[7]M. Mitomo, ''Pressure Sintering of Si_3N_4,'' *J. Mater. Sci.*, **11**, 1103–107 (1976).

[8]H. C. Yeh, W. A. Sanders, and J. L. F. Luttner, ''Pressure Sintering of Si_3N_4–Al_2O_3 (SiAlON),'' *J. Am. Ceram. Soc.*, **56** [2] 189–93 (1977).

[9]L. J. Bowen, T. G. Carruthers, and R. J. Brook, ''Hot Pressing of Si_3N_4 with Y_2O_3 and Li_2O as Additives,'' *J. Am. Ceram. Soc.*, **61** [7–8] 335–39 (1978).

[10]S.-L. Hwang and I-W. Chen, ''Reaction Hot Pressing of α′ and β′-SiAlON Ceramics,'' *J. Am. Ceram. Soc.*, **77** [1] 165–71 (1994).

[11]M. Menon and I-W. Chen, ''Reaction Densification of α′-SiAlON: I, Wetting Behavior and Acid–Base Reactions,'' *J. Am. Ceram. Soc.*, **78** [3] 545–52 (1995).

[12]M. Menon and I-W. Chen, ''Reaction Densification of α′-SiAlON: II, Densification Behavior,'' *J. Am. Ceram. Soc.*, **78** [3] 553–59 (1995).

[13]R. Drew and M. H. Lewis, ''The Microstructure of Silicon Nitride Ceramics during Hot-Pressing Transformations,'' *J. Mater. Sci.*, **9**, 261–69 (1974).

[14]D. R. Clarke and G. Thomas, ''Microstructure of Y_2O_3 Fluxed Hot-Pressed Silicon Nitride,'' *J. Am. Ceram. Soc.*, **61** [3–4] 114–18 (1978).

[15]M. H. Lewis, A. R. Bhatti, R. J. Lumby, and B. North, ''The Microstructure of Sintered Si-Al-O-N Ceramics,'' *J. Mater. Sci.*, **15**, 103–13 (1980).

[16]S.-L. Hwang and I-W. Chen, ''Nucleation and Growth of β′-SiAlON,'' *J. Am. Ceram. Soc.*, **77** [7] 1719–28 (1994).

[17]D. R. Clarke, ''Direct Observation of Lattice Planes at Grain Boundaries in Silicon Nitride''; pp. 430–40 in *Nitrogen Ceramics*. Edited by F. L. Riley. Noordhoff, Leyden, The Netherlands, 1977.

[18]C. M. Hwang, T.-Y. Tien, and I-W. Chen, ''Anisotropic Grain Growth during Final Stage Sintering of Silicon Nitride Ceramics''; pp. 1034–39 in *Sintering '87*. Edited by S. Sōmiya, M. Shimada, M. Yoshimura, and R. Watanabe. Elsevier, Essex, U.K., 1988.

[19]D. D. Lee, S. L. Kang, and D. N. Yoon, ''Mechanism of Grain Growth and α–β′ Transformation during Liquid-Phase Sintering of β′-SiAlON,'' *J. Am. Ceram. Soc.*, **71** [9] 803–806 (1988).

[20]I-W. Chen and S.-L. Hwang, ''Superplastic SiAlON—A Bird's Eye View of Silicon Nitride Ceramics;'' see Ref. 3, pp. 209–22.

[21]M. Mitomo, M. Tsutsumi, H. Tanaka, S. Uenosono, and F. Saito, ''Grain Growth during Gas Pressure Sintering of β-Silicon Nitride,'' *J. Am. Ceram. Soc.*, **73** [8] 2441–45 (1990).

[22]K.-R. Lai and T.-Y. Tien, ''Kinetics of β-Si_3N_4 Grain Growth in Si_3N_4 Ceramics Sintered under High Nitrogen Pressure,'' *J. Am. Ceram. Soc.*, **76** [1] 91–96 (1993).

[23]M. Kramer, M. J. Hoffman, and G. Petzow, ''Grain Growth Studies of Silicon Nitride Dispersed in an Oxynitride Glass,'' *J. Am. Ceram. Soc.*, **76** [11] 2778–84 (1993).

[24]M. Kramer, M. J. Hoffman, and G. Petzow, ''Grain Growth Kinetics of Si_3N_4 during α/β Transformation,'' *Acta Metall. Mater.*, **41** [10] 2939–47 (1993).

[25]L.-L. Wang, T.-Y. Tien, and I-W. Chen; unpublished work.

[26]W. W. Mullins, ''Theory of Thermal Grooving,'' *J. Appl. Phys.*, **28**, 333–39 (1957).

[27]F. A. Nichols and W. W. Mullins, ''Surface-(Interface) and Volume-diffusion Contributions to Morphological Changes Driven by Capillarity,'' *Trans. AIME*, **233** [10] 1840–48 (1965).

[28]C. F. Yen and R. L. Coble, ''Spheroidization of Tubular Voids in Al_2O_3 Crystals at High Temperatures,'' *J. Am. Ceram. Soc.*, **55** [10] 507–509 (1972).

[29]T. K. Gupta, ''Crack Healing in Thermally Shocked MgO,'' *J. Am. Ceram. Soc.*, **58** [3–4] 143 (1975).

[30]F. F. Lange and D. R. Clarke, ''Morphological Changes of an Intergranular thin Film in a Polycrystalline Spinel,'' *J. Am. Ceram. Soc.*, **65** [10] 502–506 (1982).

[31]T. Z. Chuang, K. I. Kagawa, J. R. Rice, and L. B. Sills, ''Non-equilibrium Models for Diffusive Cavitation of Grain Interfaces,'' *Acta Metall.*, **27**, 265–84 (1979).

[32]G. M. Pharr and W. D. Nix, ''A Numerical Study of Cavity Growth Controlled by Surface Diffusion,'' *Acta Metall.*, **27**, 1615–31 (1979).

[33]J. R. Porter, W. Blumenthal, and A. G. Evans, ''Creep Fracture in Ceramic Polycrystals I. Creep Cavitation Effects in Polycrystalline Alumina,'' *Acta Metall.*, **29** [12] 1899–906 (1981).

[34]M. O. Thouless and W. Linger, ''Effects of Surface and Boundary Diffusion on Void Growth,'' *Acta Metall. Mater.*, **43** [6] 2493–500 (1995).

[35]S.-L. Hwang, ''Fabrication, Microstructural Characterization, and Deformation of Superplastic SiAlON Ceramics''; Ph.D. Dissertation. University of Michigan, Ann Arbor, MI, 1992.

[36]P. Hartman, *Crystal Growth: An Introduction*. Edited by P. Hartman. North–Holland, Amsterdam, The Netherlands, 1973.

[37]J. Crank, *Mathematics of Diffusion*, Oxford University Press, Oxford, U.K., 1956.

[38]J. W. Cahn, ''On the Morphological Stability of Growing Crystals''; pp. 681–90 in *Crystal Growth*. Edited by H. S. Peiser. Pergamon Press, Oxford, U.K., 1967.
[39]W. D. Kingery, H. K. Bowen, and D. R. Uhlmann, *Introduction to Ceramics*; pp. 328–29. Wiley, New York, 1976.
[40]*Ibid*, pp. 425–30.
[41]D. R. Clarke and G. Thomas, ''Grain Boundary Phases in a Hot-Pressed MgO Fluxed Silicon Nitride,'' *J. Am. Ceram. Soc.*, **60** [11–12] 491–95 (1977).
[42]D. R. Clarke, ''High-Resolution Techniques and Applications to Nonoxide Ceramics,'' *J. Am. Ceram. Soc.*, **62** [5–6] 236–46 (1979).
[43]I. M. Lifshitz and V. V. Slyozov, ''The Kinetics of Precipitation from Supersaturated Solid Solution,'' *J. Phys. Chem. Solids*, **19** [1–2] 35–50 (1961).
[44] C. Wagner, ''Theorie der Alterung von Niederschlägen durch Umlösen (Ostwald-Reifung),'' *Z. Electrochem.*, **65**, 581–91 (1961).
[45]K. A. Jackson, ''Mechanisms of Growth''; pp. 174–86 in *Liquid Metals and Solidification*. American Society of Metals, Metals Park, OH, 1958. □